WEP Warwick Evans Publishing

International Journal of Materials Science and Technology Studies

ISSN: 3006-7693 (Print), ISSN: 3006-3744 (Online) | Volume 3, Number 2, Year 2025
DOI: https://doi.org/10.62051/ijmsts.v3n2.06
Journal homepage: https://wepub.org/index.php/IJMSTS/index

Preparation and Properties of Perovskite Solar Cells by PEAI Surface Treatment

Yunpeng Zhao, Hari Bala *, Fei Cheng, Yingjie Wen, Boji Wang

Henan Polytechnic University, Jiaozuo, China

ABSTRACT

In this study, a higher quality $MA_{0.9}FA_{0.1}PbI_{2.85}Br_{0.15}$ film was surface treated with phenylethylamine iodide (PEAI), and a perovskite solar cell (PSC) with high stability and high efficiency carbon pair electrode was prepared. The I^- and PEA^+ ions in PEAI fill the defects between the perovskite crystals, passivate the surface, improve the quality of the film, increase the size of the perovskite grains, reduce the carrier recombination, and enhance the optical properties. By comparing and testing the effect of a series of different PEAI solution concentrations on the quality of $MA_{0.9}FA_{0.1}PbI_{2.85}Br_{0.15}$ film, the optimal concentration of PEAI solution is 1.5mg /mL, and the optimal PCE of the device is 11.25%. PSCs were higher than those of untreated $MA_{0.9}FA_{0.1}PbI_{2.85}Br_{0.15}$ films. The unpackaged and PEAI solution surface treated battery devices are more stable in an air atmosphere, and the PCE of the device after 60 days remains at 96% of the initial PCE.

KEYWORDS

Perovskite solar cells; PEAI; Carbon electrode; $MA_{0.9}FA_{0.1}PbI_{2.85}Br_{0.15}$; Two-step solution spin coating process

1. INTRODUCTION

In recent years, the power conversion efficiency (PCE) of perovskite solar cells has been comparable to that of silicon-based solar cells. Despite the rapid development of PSCs in recent years, the devices prepared at room temperature have low stability and the surface topography of the devices is not very good. Therefore, it is necessary to find a suitable method to prepare the devices with high quality perovskite films, fewer grain boundaries and high carrier transmission efficiency, so as to obtain high photoelectric conversion efficiency and high environmental stability. Due to the interface characteristics between perovskite and the transport layer, defects will occur and the charge transmission will be affected. Interface engineering can effectively reduce the recombination of charge carriers at the interface by introducing passivation layers, molecular modifications, two-dimensional materials or self-assembled monolayers to optimize the surface topography [1-11]. An ultra-thin passivation layer is introduced between perovskite and the transport layer to passivate interface defects and improve charge transport, such as [6, 6] -phenyl-C61-methyl butyrate, phenethylamine iodide, etc. In addition, small molecules such as thiourea and ethylenediamine tetraacetic acid can be used to modify the surface or interface of perovskite, and the defects can be passivated by chemical bonding or physical adsorption [1, 2, 4, 12]. Introduce 2D materials (such as graphene, MoS_2) at the interface to improve charge transport and passivation defects, improve electron extraction efficiency, improve energy level matching and inhibit ion migration, or introduce metal oxides (such as Al_2O_3, TiO_2) at the interface to passivation defects, inhibit ion migration and enhance stability [9, 13-18]. Another example is MeO-2PACz, which can form a self-assembled monolayer between FTO and perovskite, thereby improving the efficiency of hole extraction,

optimization of energy level arrangement and inactivation of defects [19]. He group introduced an auxiliary chelating agent, 5, 6-isopropyridine-L-ascorbic acid (ILAA), to modify the SnO_2/ perovskite buried interface. ILAA not only inhibits SnO_2 defects and hydroxyl oxygen, but also prevents the deterioration of the perovskite layer. The introduction of ILAA optimizes the band structure of the SnO_2-perovskite interface, thus enhancing the internal electric field and promoting efficient charge transfer, and the stability is also significantly improved [20]. Different from the 3D perovskite structure, the 2D perovskite structure is to cut the 3D structure into sheets along the crystalline plane, and the larger volume of cation enters the layer to form the 2D perovskite structure, and the structural formula is also ABX_3. PEAI is often used for interface modification, and the surface of perovskite is rotated with PEAI solution to form a two-dimensional perovskite layer, which can passivate surface defects and inhibit ion migration [21-26].

The surface of the battery device is the place where defects are most easily formed, and the passivation of surface defects is always the most important task in any type of solar cell. Finding an effective passivation method for perovskite film defects can effectively improve the photoelectric conversion efficiency of perovskite solar cells. Surface passivation treatment has always been the focus of perovskite active layer research, organic halides, polymers and small molecule compounds are often used as surface passivation agents to be studied, and now the emerging multi-functional passivation agents, such as CF_3-PEAI containing trifluoromethylamine, have both hydrophobicity and strong defect passivation ability [21]. More people have focused on the interface modification of perovskite films.

The passivation layer can optimize the energy level matching between perovskite and charge transport layer to promote efficient charge extraction. The passivation of organic ammonium salt is often used, that is, the two-dimensional perovskite coating layer. Phenylethylamine iodide (PEAI) is often used as a two-dimensional perovskite material to improve the photovoltaic performance of PSCs. In this paper, PEAI is used to improve the film quality of perovskite. The ions in phenylethylamine iodide can fill the vacancy defects of the perovskite film, and PEAI and perovskite film act on the surface of the perovskite layer to form a modified layer to protect the perovskite film. In this paper, the surface of $MA_{0.9}FA_{0.1}PbI_{2.85}Br_{0.15}$ thin film was treated with different concentrations of PEAI solution, and the effects of PEAI surface modification on the crystallization properties of perovskite, the surface morphology of the thin film and the photoelectric properties of the device were investigated by various testing and characterization methods.

2. EXPERIMENTAL

2.1. Materials and Preparation

Dimethyl sulfoxide (DMSO, 99.9%), Titanium tetrachloride ($TiCl_4$, 99%), Diethanolamine (DEA, 99.9%), hydrogen peroxide (H_2O_2, 99%) and Zirconium (ZrO_2, 99.99%) were purchased from Shanghai Macklin Biochemical Co, Ltd Ltd, N-dimethylformamide (DMF, 99.8%) was purchased from Aladdin Reagent Co., LTD. Titania (TiO_2, 99.99%), FAI,PbI_2, phenethyl ammonium iodide (PEAI), MAI and $PbBr_2$ were purchased from Xian Polymer Light Technology Corp. Fluorine-doped tin oxide conductive substrates (FTO, ≤7 Ω/sq) were purchased from Shenzhen South China Xiangcheng Technology Co. Ltd. China. The carbon paste (printing ink) was purchased from Jujo Printing Supplies & Technology (Ping hu) Co. Ltd.

2.1.1. Device fabrication

The whole process of the device preparation is in the air atmosphere, the humidity is 40%-60%. The glass etched with 6mol/L hydrochloric acid is cleaned with detergent, deionized water, isopropyl alcohol and ethanol in turn, and then dried in clean air at 100℃. Then a TiO_2 (BL-TiO_2) film ($Ti(OC_4H_9)_4$: DEA: CH_3CH_2OH volume ratio) is rotated at 40000 rpm for 20s. BL-TiO_2 film was dried and annealed at 500℃ for 30 min, the substrate was treated with $TiCl_4$ solution at 70℃, and

then washed with distilled water and ethanol respectively. Mesoporous TiO_2 (ML-TiO_2) was prepared by spinning 20s at 3000 rpm. The resulting film is then dried and annealed at 500 °C for 30 minutes, cooled to room temperature, and the substrate is treated again with a diluted $TiCl_4$ solution. Then, mesoporous ZrO_2 (ML-ZrO_2) was prepared by spinning 20s at 3000 rpm.

The perovskite layer was prepared by a two-step method. The mesoporous ZrO_2 (ML-ZrO_2) layer was spin-coated with a mixture of PbI_2 and $PbBr_2$ solution, and spin-coated at 2000 r/min for 30 s. The spin-coated substrate was dried at 70℃ on the heating table for 30 min, and then cooled to room temperature. In the second step, the mixed solution of FAI and MAI was preheated at 40℃, spun at 1500 r/min for 30 s, and then the spun substrate was annealed at 100℃ for 30min and cooled to room temperature to obtain black perovskite film. Then isopropyl alcohol was used as solvent to prepare PEAI solutions with concentrations of 2mg/mL, 1.5mg/ mL, 1.0mg /mL and 0.5mg /mL, which were ultrasounded for 15min. The modified layer of perovskite film was obtained by adding 80μL of the above prepared PEAI solution, standing for 8s and spinning at a speed of 4000 r/min for 20 s. The carbon electrode was then scraped and coated with carbon paste and dried at 100 ℃ for 15 min. The effective area of the device was 0.1cm². The battery structure is shown in Figure 1

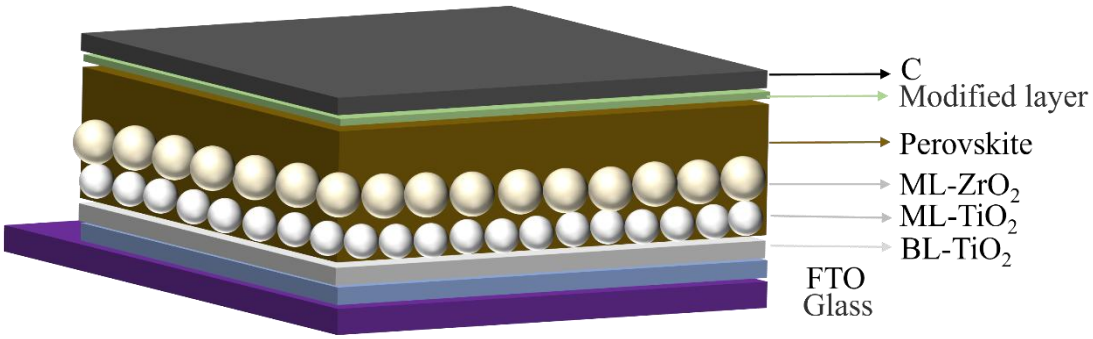

Figure 1. Structure of perovskite solar device

2.2. Characterization

The surface morphology of perovskites was first observed using scanning electron microscopy (SEM, Carl Zeiss Microimaging GmbH, Germany). Micro - and nano-scale topography observation and in situ spm imaging were performed by the nanomechanical Properties testing System (Hysitron Instruments, Inc.). The scanning imaging rate of SPM imaging was 0.5Hz, the setting force was 2mN, and the scanning size was 10μm. X-ray diffractometer (Rigaku Corporation, Japan) was used to measure the diffraction Angle and intensity to determine the crystal structure, lattice parameters and phase composition of the material. With TU-1810PCS UV-Vis spectrophotometer, the structure of the compound was determined and the properties of the compound were characterized. With glass with FTO as a blank control group, the absorption spectra of perovskite films were determined by spectrophotometer with the range of 400-900 nm. The photoluminescence (PL) spectrum of photoinduced luminescence was then measured using a steady-state fluorescence spectrometer (Edinburgh FLS1000) with a test range of 650-850 nm and an excitation wavelength of 467 nm. Solar simulator BOS-X-1000G was used to test the prepared device, and the irradiance was 100mW/cm^2, equivalent to the solar radiation under the spectrum of AM1.5G. keithley2602-A digital power meter was used to apply bias voltage to both ends of the solar cell for scanning, and the current value of its external circuit was measured. The J-V characteristic curve is obtained.Electrochemical workstation (CHI660E B193227, Co., LTD.) was used to measure the electrochemical impedance profile of PSCs in the frequency range of 100MHz-100kMHz with a bias of 0.1V. Then the water resistance of perovskite active layer was studied by using a contact Angle measuring instrument (Dhhv1351UM). The suspension drop method was used to measure the water resistance. The contact Angle measuring range was $0<\theta<180°$.

3. RESULTS AND DISCUSSION

3.1. Surface Topography Analysis

In order to study the effect of different concentrations of PEAI on the surface morphology of $MA_{0.9}FA_{0.1}PbI_{2.85}Br_{0.15}$ films after surface treatment, $MA_{0.9}FA_{0.1}PbI_{2.85}Br_{0.15}$ films treated with different concentrations of PEAI were prepared under air atmosphere, and a series of devices were prepared using carbon as the counter electrode. The crystal morphology of perovskite thin film surface was observed by SEM and SPM, and the results were shown in Figure 2.

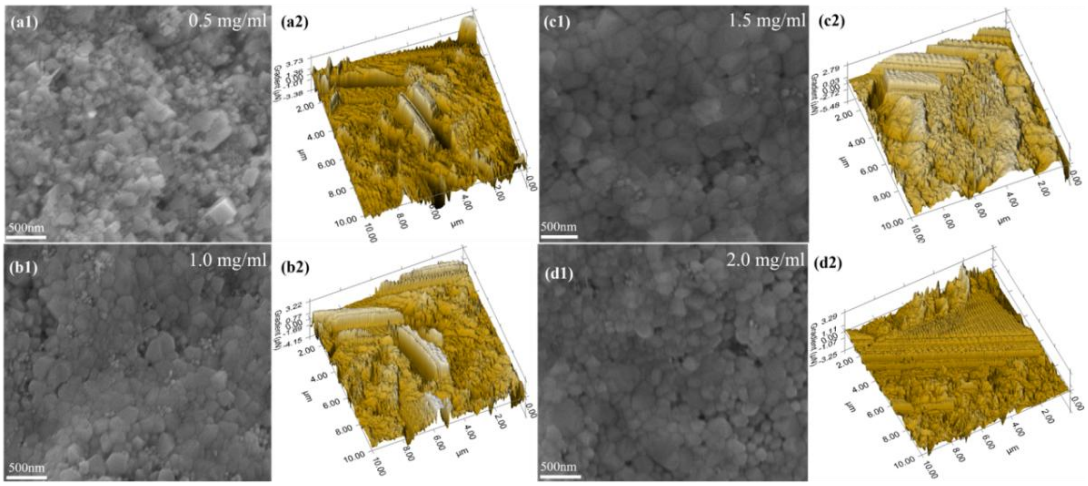

Figure 2. Surface SEM and SPM images of (a) 0.5mg /mL, (b) 1.0mg /mL, (c) 1.5mg /mL and (d) 2.0mg /mL PEAI treated $MA_{0.9}FA_{0.1}PbI_{2.85}Br_{0.15}$ films

Figure 2 (a) shows the morphology of $MA_{0.9}FA_{0.1}PbI_{2.85}Br_{0.15}$ perovskite film modified by 0.5mg /mL PEAI interface. It can be seen from the figure that perovskite crystals are not tight, and perovskite crystals are mostly cubic structure. The surface morphology of the film is not good, with large roughness and excessive grain boundaries. Because the grain size is too small, it is easy to cause carrier recombination at these defects, which hinders carrier transmission and is not conducive to the improvement of device performance. The consideration is that because the concentration of PEAI is too low, the effect of improving surface defects is not obvious. Figure (b) shows the morphology of $MA_{0.9}FA_{0.1}PbI_{2.85}Br_{0.15}$ perovskite film modified with 1.0mg /mL PEAI interface. Compared with Figure a, it can be clearly seen that the surface morphology of perovskite has been improved, crystal quality has been improved, grain boundaries have been reduced, crystal size has been increased, and the crystal connection between crystals is closer than that in Figure a. But there are still large areas of defects. Figure (c) shows the morphology of perovskite film modified with 1.5mg /mL PEAI interface. It can be clearly seen from the above figure that the grain size increases, the grain boundaries decrease, and the connection between grains becomes closer. Compared with the previous two, the surface morphology of perovskite film has been improved. After 1.5 mg/mL PEAI interface modification, it is beneficial to improve the carrier transport of perovskite films, so as to obtain better performance. While Figure (d) shows the morphology of the perovskite film modified with 2.0mg /mL PEAI interface. It can be seen from the above figure that the grain size decreases, the grain boundaries increase, the surface of the film is not flat, and the arrangement between the crystals is not very tight compared with Figure c. The increase of the concentration cannot continue to improve the surface morphology of the film. Therefore, after the modification of $MA_{0.9}FA_{0.1}PbI_{2.85}Br_{0.15}$ film with 1.5mg/mL PEAI solution, the perovskite has the largest grain size, the least grain boundaries and the best surface morphology.

3.2. Crystal Structure and Properties Descriptions

To further explore the effects of PEAI solution with different concentrations on the phase purity and crystallization properties of perovskite thin films, X-ray diffraction analysis was performed on the perovskite thin films obtained after surface treatment with different concentrations of PEAI, and the XRD patterns obtained were shown in Figure 3:

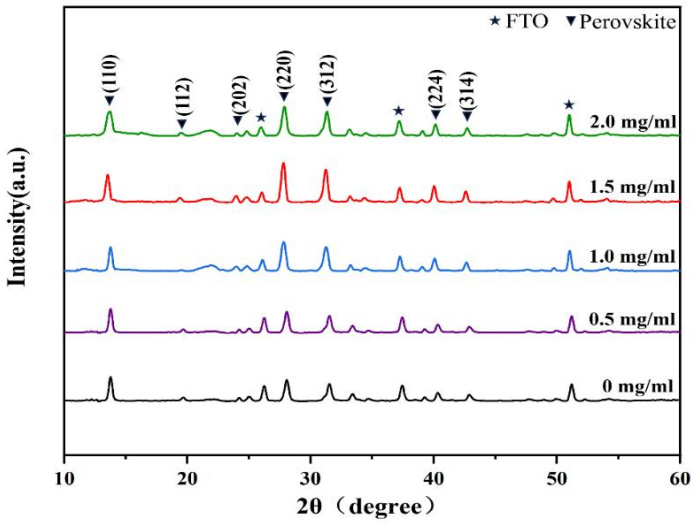

Figure 3. XRD patterns of perovskite films treated with different concentrations of PEAI

After a small concentration of PEAI solution modified the surface of the perovskite film, no new peaks were found compared with the XRD pattern, indicating that a small amount of PEAI solution did not cause changes in the crystal pattern of perovskite, and no other impurity peaks were introduced. It can be seen from the above figure that the three most significant diffraction peaks formed at 2θ of 13.5°, 27.8° and 31.4° are characteristic peaks of perovskite, corresponding to the (110), (220) and (312) crystal faces of perovskite, respectively. After the interface modification of perovskite film by PEAI, the characteristic peak is significantly enhanced compared with the perovskite without rotational PEAI coating, but the peak position does not shift, indicating that the crystallinity of perovskite is improved. Compared with the perovskite films without PEAI treatment, the diffraction peaks of the films treated with PEAI are enhanced at 27.8°. The diffraction peak intensity of $MA_{0.9}FA_{0.1}PbI_{2.85}Br_{0.15}$ perovskite film after PEAI treatment with a concentration of 1.5mg /mL is the highest, indicating that its crystallization performance is the best, which corresponds to the scanning image measured by us before. However, when the concentration continued to increase, the crystallization performance of perovskite did not improve, on the contrary, the strength of the diffraction peak decreased, considering that the concentration of PEAI solution was too large, resulting in the reduction of perovskite grain size, the increase of defects, and the reduction of film coverage. Finally, we concluded that when the concentration of PEAI is 1.5 mg/mL, the surface modification of $MA_{0.9}FA_{0.1}PbI_{2.85}Br_{0.15}$ perovskite film can obtain the best effect. Corresponding to the scan results, we also conducted a series of characterization tests to explore the accuracy of this conclusion.

3.3. Optical Performance Descriptions

In order to explore the effects of PEAI interface modification on the optical properties of perovskite films, UV-V is absorption spectra of $MA_{0.9}FA_{0.1}PbI_{2.85}Br_{0.15}$ perovskite films modified with different concentrations of PEAI were analyzed. The test results are shown in Figure 4 below.

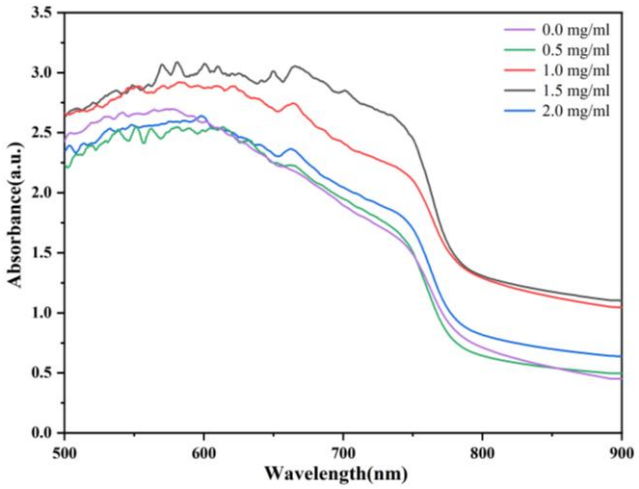

Figure 4. Absorption spectra of $MA_{0.9}FA_{0.1}PbI_{2.85}Br_{0.15}$ films treated with different concentrations of PEAI

As shown in Figure 4, the ultraviolet light absorption intensity of the perovskite film corresponding to the five curves showed a violent increase at about 800 nm, and the light absorption intensity of the perovskite film after PEAI treatment was higher than that of the unmodified perovskite film. When the concentration of PEAI solution is 1.5mg /ml, the light absorption intensity is the highest, and the light absorption edge is the steepest, which indicates that the crystallization property of the film is better, the grain boundary is less, the grain size is larger, and the quality of the perovskite film is the highest. We found that after the surface modification treatment of the film surface with PEAI solution, the light absorption edge did not move significantly, indicating that the band gap of the perovskite film after PEAI treatment did not change. However, when the concentration of PEAI continues to increase, the absorbance of perovskite film decreases. When the concentration of PEAI is 2.0 mg/ml, the absorbance decreases significantly, which corresponds to the XRD analyzed previously. Therefore, we can conclude that after the surface treatment of perovskite film with 1.5 mg/mL PEAI, the absorbance of perovskite film decreases significantly. The optical properties of $MA_{0.9}FA_{0.1}PbI_{2.85}Br_{0.15}$ film are obviously improved, the crystal size is the largest, the grain boundary is reduced, and the film quality is the best.

The combination of electrons and holes produced by perovskite films under light can be understood by the steady-state photoluminescence spectra. Therefore, PL spectra of $MA_{0.9}FA_{0.1}PbI_{2.85}Br_{0.15}$ perovskite films modified with different concentrations of PEAI were analyzed, as shown in Figure 5.

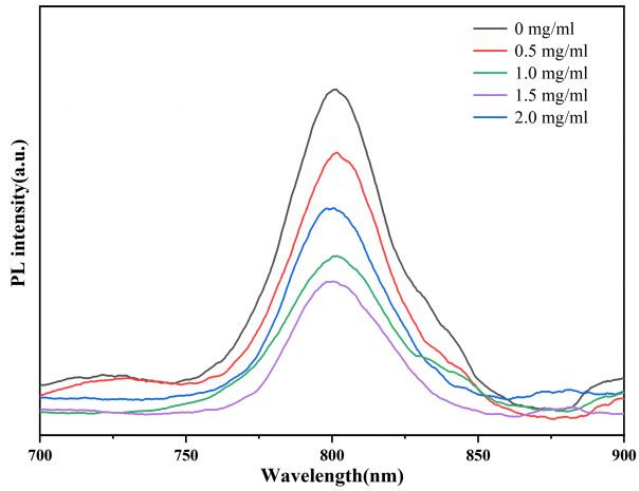

Figure 5. Steady-state emission fluorescence spectra of $MA_{0.9}FA_{0.1}PbI_{2.85}Br_{0.15}$ perovskite films treated with different concentrations of PEAI

It can be seen from Figure 5 that the peak photoluminescence intensity of perovskite thin films is around 800 nm, and this result is consistent with the light absorption edge in the above absorption spectrum. After surface modification treatment with PEAI solution, the photoluminescence intensity of perovskite thin films is weakened. The untreated films have the highest PL peak value, which indicates that after interface treatment, the quality of $MA_{0.9}FA_{0.1}PbI_{2.85}Br_{0.15}$ films is improved, the recombination of electrons and holes is relatively small, the non-radioactive recombination is less, and the surface defects of perovskite films are reduced. The film PL peak value after 1.5 mg/ml treatment is the lowest, indicating that the film surface quality is the best, which corresponds to our previous conclusion.

3.4. Photoelectric Conversion Performance

In order to investigate the effect of surface modification treatment on the surface of $MA_{0.9}FA_{0.1}PbI_{2.85}Br_{0.15}$ thin film with different PEAI solutions on the photoelectric conversion efficiency and photovoltaic performance of perovskite solar cell devices, simulated sunlight (AM 1.5G, 100 $mW \cdot cm^{-2}$) was used as the light source. A series of carbon electrode devices are prepared, and the test results are shown in the following figure. The detailed photovoltaic performance parameters are shown in the following table.

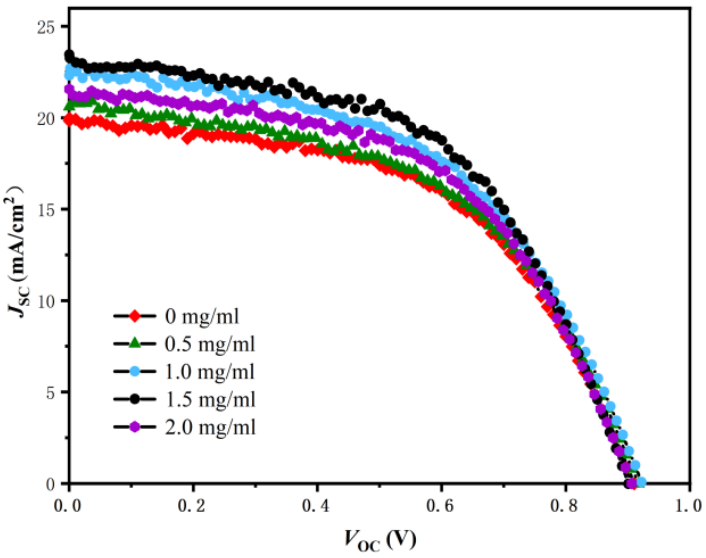

Figure 6. J-V characteristic curves of PSCs treated with PEAI at different concentrations under AM 1.5G (100mW·cm^{-2}) simulated sunlight irradiation

Table 1. Detailed photovoltaic performance parameters of the device after surface modification

PEAI concentration	VOC (mV)	JSC (mA·cm^{-2})	FF	PCE (%)
0 mg/ml	910	19.82	0.53	9.63
0.5 mg/ml	917	20.60	0.52	9.79
1.0 mg/ml	921	22.31	0.52	10.76
1.5 mg/ml	908	23.44	0.53	11.25
2.0 mg/ml	906	21.56	0.53	10.37

From the table, we can see that the voltage change of the overall device is not very large, and the current has changed. Among them, the efficiency of the device without PEAI surface treatment is 9.63%, while the efficiency of the device after interface treatment is improved. With the increase of the concentration, the photoelectric conversion efficiency of the device is also improved. When the PEAI concentration is 1.5 mg/ml, the highest PCE is obtained, which is 11.25%. After interface

modification, I^- and PEA^+ in PEAI solution filled the vacancy defect on $MA_{0.9}FA_{0.1}PbI_{2.85}Br_{0.15}$ film, and the performance of the device was significantly enhanced, mainly because the quality of the perovskite film was improved and the carrier recombination was reduced. When the concentration continues to increase, the PCE of the device begins to decline, which may be due to the reduction of grain size, the increase of grain boundaries, the decrease of film quality, and the reduction of internal carrier transmission after the treatment of excessive PEAI solution, resulting in a decrease in efficiency. When the PEAI concentration is 1.5 mg/ml, the optical properties of perovskite films are improved, and the devices have the best photoelectric conversion efficiency, which corresponds to the conclusions of our previous tests.

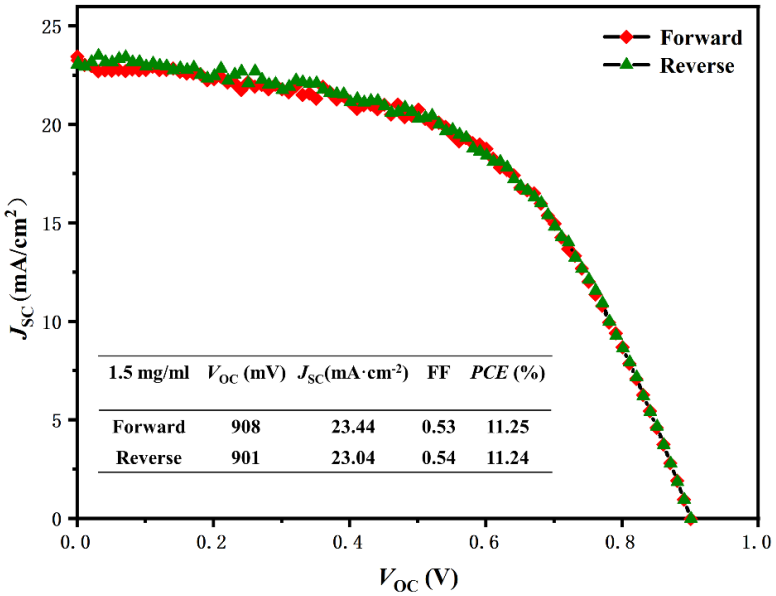

1.5 mg/ml	V_{OC} (mV)	J_{SC}(mA·cm^{-2})	FF	*PCE* (%)
Forward	908	23.44	0.53	11.25
Reverse	901	23.04	0.54	11.24

Figure 7. Forward and reverse scanning J-V characteristic curves of PSCs treated with 1.5mg /mL PEAI solution

Figure 7 shows the *J-V* characteristic curves of forward and reverse scanning of PSCs after the $MA_{0.9}FA_{0.1}PbI_{2.85}Br_{0.15}$ film was treated with 1.5mg /mL PEAI solution. It can be seen from the figure that there is no significant difference in photovoltaic performance parameters between the forward and reverse scanning devices, with a 7mV difference in *Voc*. *Jsc* differed by 0.4 mA·cm^{-2}, FF by 0.01, and *PCE* by 0.01%. Hysteresis effect reflects the charge recombination and ion migration inside the device, and there is no obvious hysteresis phenomenon in the prepared device, which is because the I^- and PEA^+ ions in PEAI fill the vacancy defect in $MA_{0.9}FA_{0.1}PbI_{2.85}Br_{0.15}$. After the interface modification of PEAI solution, the crystal size of perovskite increases. The surface defect density is reduced, the recombination between carriers is reduced, and the light trapping ability is improved. The coincidence degree of the two curves of forward scan and reverse scan is highly consistent, which also proves that the device modified by PEAI solution interface has excellent photovoltaic performance, which is also consistent with our previous test characterization.

3.5. Electrochemical Analysis of Device Internals

An electrochemical workstation was used to test the electrochemical impedance of PSCs composed of $MA_{0.9}FA_{0.1}PbI_{2.85}Br_{0.15}$ thin films treated with PEAI at different concentrations. Figure 8 shows the Nyquist spectrum measured when the bias voltage of the device is 0.1V, and the figure below shows the equivalent circuit model diagram corresponding to PSCs.

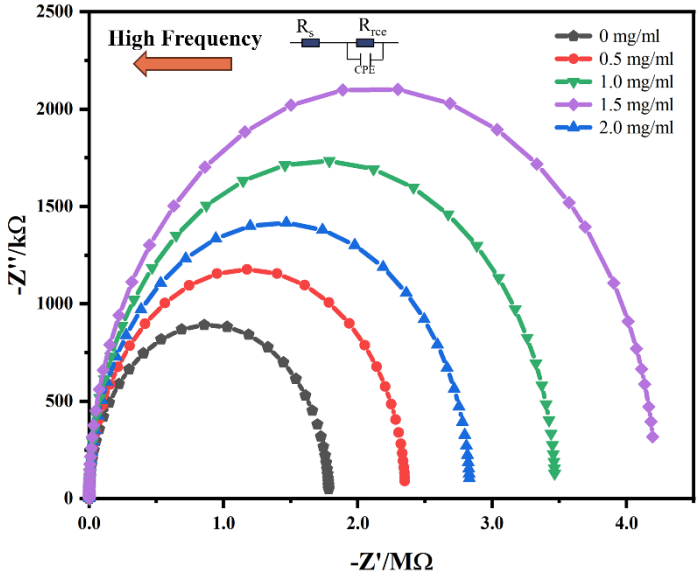

Figure 8. Electrochemical impedance diagram of PSCs treated with different concentrations of PEAI

In Figure 8, the starting point of the semicircle of the impedance diagram corresponds to the series resistance (R_s). Since the prepared PSCs have the same structure, they have similar R_s values, so the starting point of the semicircle is basically the same. The size of the semicircle is proportional to the equivalent composite resistance (R_{rce}) in the device, the larger the radius of the semicircle, the larger the R_{rce} will be, and the larger the R_{rce}, the greater the hindrance of the carrier recombination inside the device, and the higher the carrier transmission efficiency. It can be seen from the figure that the semi-circle of the device without PEAI treatment is the smallest, indicating that the smaller the composite resistance, the easier it is for the carrier to recombine inside the device. After PEAI processing, the figure reflects that the radius of the semicircle is larger, indicating that the R_{rce} is larger, and the carrier is less likely to recombine. After the PEAI concentration is 1.5 mg/ml, the radius of the semicircle is the largest, indicating that there is the largest R_{rce}, and the loss caused by the recombination of carriers is the least, the photoelectric parameters will be improved, and the photoelectric characteristics will be better, which is also corresponding to the conclusions we obtained in the previous chapter.

3.6. Stability Analysis

The stability of perovskite batteries in the environment is particularly important, which is an important indicator of whether it can be applied on a large scale, we know from the above that perovskite will decompose when exposed to water in the air for a long time. In order to explore the stability of PEAI surface treated devices, testing the size of the contact Angle between the devices and water can reflect the quality of its hydrophobicity. We prepared PSCs with carbon pair electrode, and tested the effect of PEAI modification on the device hydrophobicity within 5min in air atmosphere. The test results are shown in Figure 9.

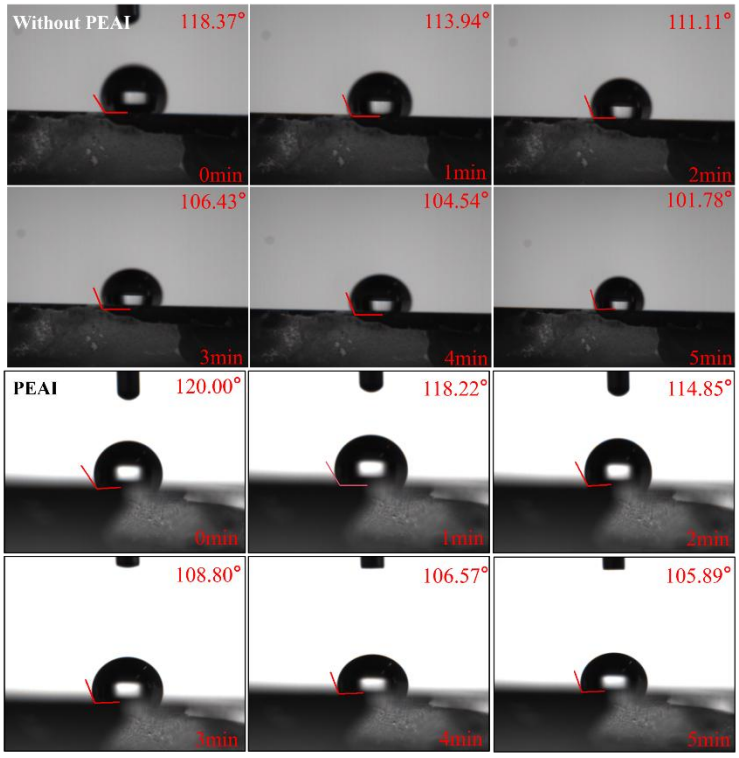

Figure 9. Contact Angle changes of PSCs with or without PEAI modified carbon electrode and water at 0, 1, 2, 3, 4 and 5 min

When water touches the surface of the PEAI-modified device, the contact Angle is 120°, which is higher than the 118.37° of the unmodified device, and after a minute change, the surface perovskite reacts and decomposes with water, and the contact Angle of the modified device is reduced to 118.22°, which is also higher than the 113.94° of the unmodified device. At the 5th minute, the angles were 105.89° and 101.78° respectively. Due to the surface modification of the perovskite film to form a protective layer, the contact Angle of the modified device was greater than that of the unmodified device, and the quality of the modified perovskite film was improved. This also corresponds to our test characterization in the previous section. The contact Angle of both of them is greater than 90° within 5 min, indicating that PSCs with carbon electrode can still maintain hydrophobicity after contact with water for a period of time. The use of carbon electrodes can block the erosion of water molecules on the device. After PEAI treatment, the hydrophobic property of $MA_{0.9}FA_{0.1}PbI_{2.85}Br_{0.15}$ film is improved, and the synergistic effect with carbon electrode can improve the long-term stability of the device.

A device with a thin film of $MA_{0.9}FA_{0.1}PbI_{2.85}Br_{0.15}$ and modified by 1.5 mg/ml PEAI was prepared in the whole process under air atmosphere. Unpackaged stability test was carried out to test the changes of various photoelectric performance parameters (*Voc*, *Jsc*, FF and *PCE*) within 60 days. The results are shown in Figure 10 below.

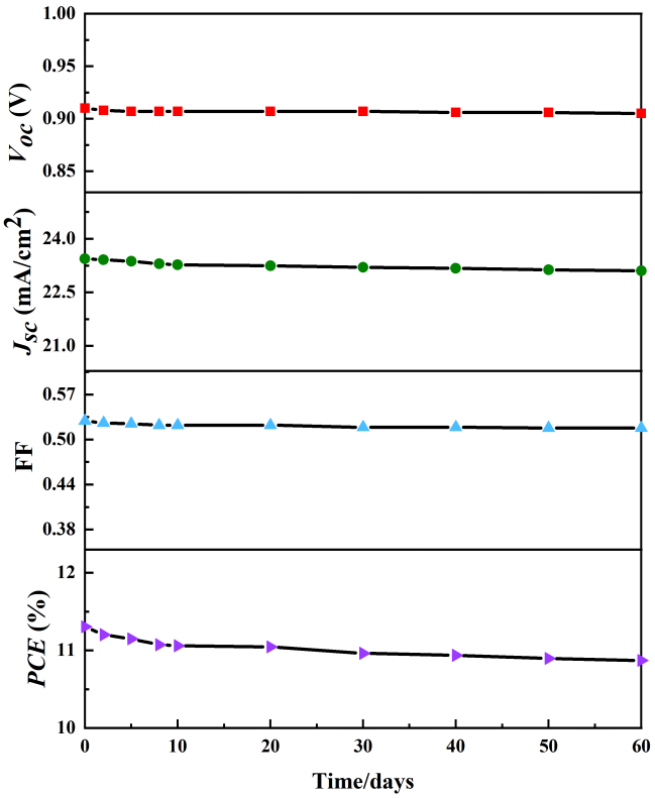

Figure 10. The change curve of the photoelectric parameters of the optimal device after 60 days in an air atmosphere

It can be seen from Figure 10 that after 60 days of changes, the V_{OC} of the device has remained relatively stable. J_{SC} and FF decreased slightly in the first 10 days due to the influence of environmental factors, resulting in a small decrease in the PCE of the device, and then tended to be stable. This is mainly due to high quality modified perovskite films and carbon electrodes with good water resistance. After 60 days of aging, the efficiency of the device has decreased slightly, but it is still 96% of the initial PCE. It shows good long-term stability.

4. SUMMARY

In this paper, $MA_{0.9}FA_{0.1}PbI_{2.85}Br_{0.15}$ thin films were prepared by two-step solution spin coating method under air atmosphere, and PSCs with the structure of FTO/TiO_2 compact layer /TiO_2 mesoporous layer /ZrO_2 mesoporous layer/perovskite layer /PEAI modified layer/carbon electrode were prepared. The surface of the perovskite film was treated, and the influence of different concentrations of PEAI on the $MA_{0.9}FA_{0.1}PbI_{2.85}Br_{0.15}$ film and the overall performance of the device was studied. By comparing different concentrations of PEAI solution in this chapter, the best perovskite film was obtained by treating $MA_{0.9}FA_{0.1}PbI_{2.85}Br_{0.15}$ film with PEAI solution with concentration of 1.5 mg /mL, which has the best film quality, the best optical properties and the best photoelectric parameters. The highest PCE obtained was 11.25%. Through microscopic observation of the PEAI treated $MA_{0.9}FA_{0.1}PbI_{2.85}Br_{0.15}$ film, it is found that the interface treatment of $MA_{0.9}FA_{0.1}PbI_{2.85}Br_{0.15}$ film with suitable PEAI solution can reduce the grain boundary of the crystal cell, improve the crystallinity and reduce the defects. The recombination of internal carriers is reduced and the photoelectric conversion efficiency of the device is enhanced. $MA_{0.9}FA_{0.1}PbI_{2.85}Br_{0.15}$ films treated with 1.5 mg /mL PEAI showed good hydrophobicity and environmental stability. The device prepared in air atmosphere has good long-term stability in the 60-day stability test, and can still maintain 96% of the initial efficiency, indicating that the surface treatment can improve its long-term stability.

REFERENCES

[1] HAIFEI W, SHUOJIAN S, YUETIAN C, et al. Impurity-healing interface engineering for efficient perovskite submodules [J]. Nature, 2024.

[2] KUMAR A, SINGH S, SHARMA A, et al. Efficient and stable perovskite solar cells by interface engineering at the interface of electron transport layer/perovskite [J]. Optical Materials, 2022.

[3] LIU Z, LI H, CHU Z, et al. Reducing Perovskite/C60 Interface Losses via Sequential Interface Engineering for Efficient Perovskite/Silicon Tandem Solar Cell [J]. Advanced Materials, 2023.

[4] NIU G, LI W, LI J, et al. Progress of interface engineering in perovskite solar cells [J]. Science China Materials, 2016.

[5] YU W, SUN X, XIAO M, et al. Recent advances on interface engineering of perovskite solar cells [J]. Nano Research, 2021.

[6] ZHAO C, ZHANG H, KRISHNA A, et al. Interface Engineering for Highly Efficient and Stable Perovskite Solar Cells [J]. Advanced Optical Materials, 2023.

[7] GUO X, ZHANG B, LIN Z, et al. Interface engineering of TiO2/perovskite interface via fullerene derivatives for high performance planar perovskite solar cells [J]. Organic Electronics, 2018.

[8] HEO D Y, JANG W J, JEONG M J, et al. Optimal Solvents for Interfacial Solution Engineering of Perovskite Solar Cells [J]. Solar RRL, 2022.

[9] QIU L, SI G, BAO X, et al. Interfacial engineering of halide perovskites and two-dimensional materials [J]. Chemical Society Reviews, 2022.

[10] SHEN G, CAI Q, DONG H, et al. Using Interfacial Contact Engineering to Solve Nickel Oxide/Perovskite Interface Contact Issues in Inverted Perovskite Solar Cells [J]. ACS Sustainable Chemistry & Engineering, 2021.

[11] TAVAKOLI M M, SALIBA M, YADAV P, et al. Synergistic Crystal and Interface Engineering for Efficient and Stable Perovskite Photovoltaics [J]. Advanced Energy Materials, 2018.

[12] GAO W, LI P, CHEN J, et al. Interface Engineering in Tin Perovskite Solar Cells [J]. Advanced Materials Interfaces, 2019.

[13] CAMMARATA A, RONDINELLI J M. Electronic doping of transition metal oxide perovskites [J]. Applied Physics Letters, 2016.

[14] CHEN J, MORROW D J, FU Y, et al. Single-Crystal Thin Films of Cesium Lead Bromide Perovskite Epitaxially Grown on Metal Oxide Perovskite (SrTiO3) [J]. Journal of the American Chemical Society, 2017.

[15] LAN C, ZHOU Z, WEI R, et al. Two-dimensional perovskite materials: From synthesis to energy-related applications [J]. Materials Today Energy, 2018.

[16] MIAO S, LIU T, DU Y, et al. 2D Material and Perovskite Heterostructure for Optoelectronic Applications [J]. Nanomaterials, 2022.

[17] UM KANTA A, MEHRAD A, VIDA T, et al. 2D materials for organic and perovskite photovoltaics [J]. Nano Energy, 2021.

[18] YOU P, TANG G, YAN F. Two-dimensional materials in perovskite solar cells [J]. Materials Today Energy, 2018.

[19] TING J, YAJIE Y, XIA H, et al. Self-Assembled Monolayer Hole Transport Layers for High-Performance and Stable Inverted Perovskite Solar Cells [J]. Energy & Fuels, 2024.

[20] HE Z, ZHANG S, WEI Q, et al. Making a benign buried bottom interface for high-performance perovskite photovoltaics with a chelating molecule [J]. Nano Energy, 2024.

[21] JUNJIE Z, MINGHAO L, SIYANG W, et al. 2-CF3-PEAI to eliminate Pb0 traps and form a 2D perovskite layer to enhance the performance and stability of perovskite solar cells [J]. Nano Energy, 2022.

[22] LI M, ZHOU J, TAN L, et al. Brominated PEAI as Multi-Functional Passivator for High-Efficiency Perovskite Solar Cell [J]. Energy & Environmental Materials, 2022.

[23] WANG Y-F, LIU Y-F, ZHANG H-W, et al. Enhanced efficiency and stability of perovskite solar cells through nanoimprinting dual-functional nanostructured PEAI/2D/3D perovskite interface [J]. Chemical Engineering Journal, 2024.

[24] WU R-J, WU K-T, NIAN G-H, et al. Preparation and characterization of low-dimensional MAPbI3 perovskite nanowires with enhanced photoluminescence and photoresponsive properties by incorporating PEAI [J]. Journal of Physics and Chemistry of Solids, 2022.

[25] XU C, ZHANG Z, HU Y, et al. Printed hole-conductor-free mesoscopic perovskite solar cells with excellent long-term stability using PEAI as an additive [J]. Journal of Energy Chemistry, 2018.

[26] ZHU T, ZHENG D, LIU J, et al. PEAI-Based Interfacial Layer for High-Efficiency and Stable Solar Cells Based on a MACl-Mediated Grown FA0.94MA0.06PbI3 Perovskite [J]. ACS Applied Materials & Interfaces, 2020.